

# Journal of Applied Sciences

ISSN 1812-5654





# **Dynamic Analysis of Esfahan Metro Tunnels**

A. Bagherzadeh and B. Ferdowsi Rock Mechanics Engineering Division, Department of Mining Engineering, Sahand University of Technology, Tabriz, Iran

**Abstract:** This study discusses the modeling of Esfahan metro tunnels subjected to earthquake and interaction of tunnels. In critical structures like subway tunnels, performing a time history dynamic analysis is the only acceptable method for determining the seismic-induced forces. For sites with no recorded earthquake ground motion, artificially generated accelerograms to represent the real earthquake records has been suggested by many experts. This study addressed the modeling of metro tunnels subjected to earthquake with finite difference numerical model. FDM model is developed to estimate the long-term support system. The numerical results of obtained in this research were compared with the analytical solutions. The analytical procedure in this study is limited in scope; it appears to be useful for a preliminary design of tunnel linings to estimate the seismic effect.

Key words: Urban tunneling, numerical methods, analytical methods, tunnel support, seismic loading

### INTRODUCTION

In modern urban areas, underground facilities, including subways, underground rail and road tunnels, underground storage tanks and common utility ducts, are essential to human life. Hence, in critical structures like subway tunnels, performing a time history dynamic analysis is the only acceptable method for determining the seismic-induced forces.

Underground structures are generally considered less vulnerable to seismic loading than above ground structures. However, even if dynamic effects are small, response of underground structures may inflict significant loads on the support system, which have to be included.

Esfahan is one of the largest and most well known cities in Iran. With the rapid economic development and reform of the last two decades, construction activities of civil infrastructures and buildings in the Municipality of Esfahan have been increasing significantly. North-south line has 15 stations and a total length of 12.5 km, which comprises a 12 km long underground tunnel. The underground tunnels have horseshoe cross sections. The twin tunnels excavation discussed in this study is located between Azadi Station and Soffeh Station (Fig. 1). Underground structures do not fall in resonance with the ground but react in accordance with the reflex of the surrounding ground.

Although, generally, underground structures exhibit a better performance than surface structures, in some situations they may be particularly vulnerable to seismic

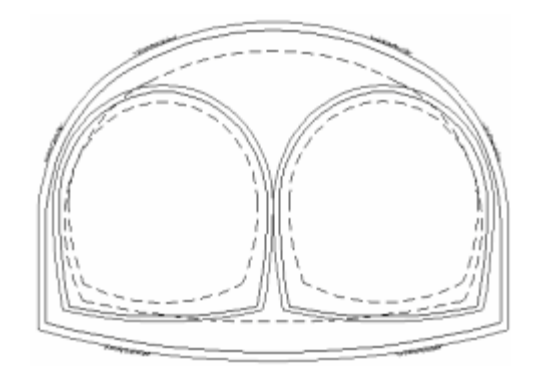


Fig. 1: Cross-sectional sketches of Esfahan metro tunnels

loading depending on: (1) the size, shape and depth of underground structure; (2) the geotechnical ground conditions and (3) the severity of ground shaking (St John and Zahrah, 1987).

### DEFINITION OF SEISMIC ENVIRONMENT

Regardless of the qualitative characterizations of earthquake, an engineer concerned with design of underground structures requires that the seismic environment be defined in a quantitative manner.

Specifically, the characteristics of earthquakes and ground movement pertinent to the development of seismic input criteria are the size of the earthquake, the intensity and the frequency content of the ground motion and the

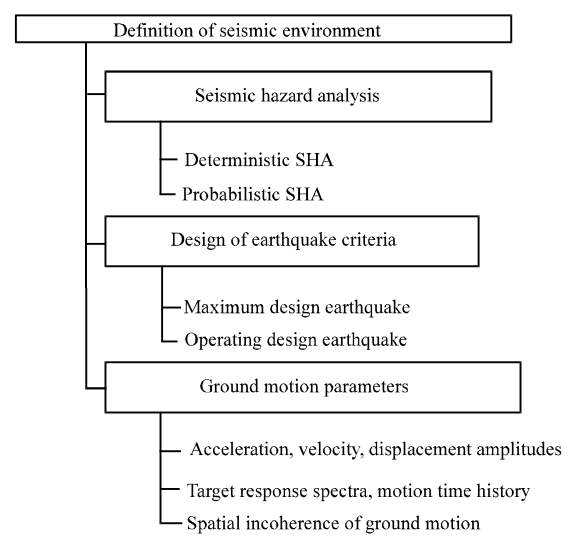


Fig. 2: Development of the seismic parameters procedure (Hashash *et al.*, 2001)

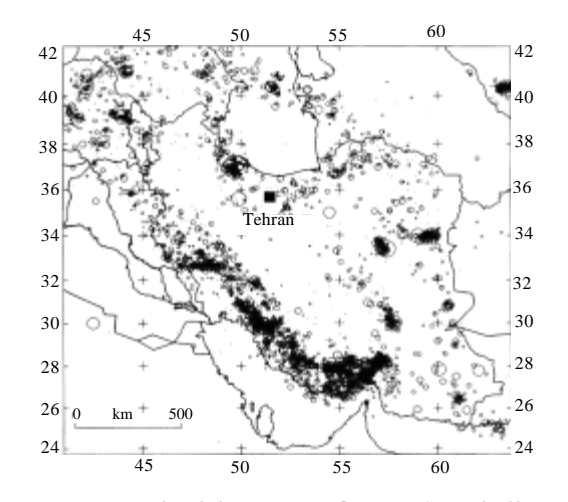


Fig. 3: Recent seismicity map of Iran (Tavakoli and Ashtiany, 1999; Amiri et al., 2003)

duration of strong shaking (St John and Zahrah, 1987). Therefore, the assessment of underground structure seismic response requires an understanding of the anticipated ground shaking as well as an evaluation of the response of the ground and the structure to such shaking. Figure 2 shows a systematic procedure for evaluating the seismic environment and development of the seismic parameters for analysis (Hashash *et al.*, 2001).

Iran is one of the most seismic countries of the world. It is situated over the Himalayan-Alpied seismic belt and is one of those countries which have lost many human lives and a lot of money due to the occurrence of earthquakes. Figure 3 shows the recent seismicity of Iran (Tavakoli and Ashtiany, 1999). In this country, a destructive earthquake occurs every several years due to the fact that it is situated over a seismic zone.

The aim of earthquake-resistant design for underground structures is to develop a facility that can resist a given level of seismic action with damage not exceeding a pre-defined acceptable level. The design level of shaking is typically defined by a design ground motion, which is characterized by the amplitudes and characteristics of expected ground motions and their expected return frequency (Kramer, 1996). A Seismic Hazard Analysis (SHA) is used to define the level of shaking and the design earthquake(s) for an underground structure.

In order to find the base design acceleration of a site, one customary method is based on seismic hazard analysis. In this method, the base design acceleration is derived from seismic activity of the region, ground type, attenuation relationships and use of statistical and probabilistic methods. One of the essential components of this method is existence of suitable attenuation relationships for different parameters (Tavakoli and Ashtiany, 1999). There are two methods of SHA: (a) the deterministic seismic hazard analysis (DSHA) and (b) the probabilistic seismic hazard analysis (PSHA) (Hashash *et al.*, 2001).

A DSHA develops one or more earthquake motions for a site, for which the designers then design and assess the underground structure. The more recent PSHA, which explicitly quantifies the uncertainties in the analysis, develops a range of expected ground motions and their probabilities of occurrence (Hashash *et al.*, 2001). These probabilities can then be used to determine the level of seismic protection in a design.

Ground-motion parameters: In order to be of use to the engineer, the severity of ground motion must be quantified concisely whilst retaining the important damage-inducing characteristics of the earthquake record. There are many ways of doing this, based on time histories of ground motion, although no single parameter is considered sufficient to accurately explain all of the significant ground-motion characteristics (Kramer, 1996). For earthquake engineering applications, amplitude, frequency, duration and energy content are the strong-motion characteristics of most interest.

The commonest measure of the amplitude of earthquake motion is the peak ground acceleration (PGA). Though accelerations are related directly to inertial forces, PGA itself is not a particularly good measure of damage to structures, except in certain special cases (i.e., very stiff structures).

Velocity is a parameter less sensitive to high frequency components of the ground motion. As such, the peak ground velocity (PGV) is a helpful component of the effect of ground motion on structures such as tall or

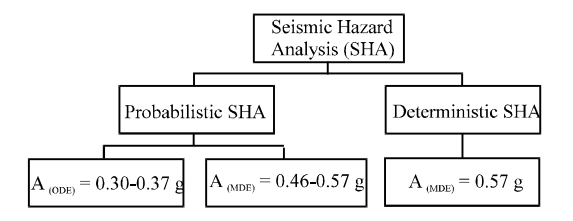


Fig. 4: Results of seismic hazard analysis

flexible buildings, which are sensitive to intermediate frequencies. Velocity parameters in general are closely linked to the energy associated with an earthquake record, so may be better indicators of structural damage potential (Newmark and Hall, 1982).

Peak ground displacements (PGD) are related more to the low-frequency content of strong ground motion. Where, displacements are calculated from the integration of acceleration time-histories, their reliability in characterizing aspects of the true ground motion is significantly limited by inaccuracies in processing the raw data and by the presence of long period noise. PGA, PGV or PGD normally refer to the maximum amplitudes of motion as measured in the horizontal plane. The peak ground-motion amplitudes in the vertical plane are usually lower than those measured in the horizontal plane (Hashash *et al.*, 2001).

The selected accelerogram for this area has a peak acceleration of about 0.57 g. Figure 4 shows the results of seismic hazard analysis for evaluating the seismic environment and development of the seismic parameters.

# NUMERICAL APPROACH

To study the seismic response of underground structures, a forceful computer code is to be used. The computer code has to have the ability to incorporate key factors and phenomena that influence the behavior of unimproved and improved ground. The flexibility of the computer code for alternative soil models has to be taken into account.

In this study the numerical models perform a time domain analysis under absorbing boundaries to simulate a semi-infinite medium.

**Geotechnical parameters of the model:** The material properties of the lined tunnel, soil and earthquake properties are given in Table 1. Figure 5 shows Numerical model and boundary condition for dynamic analysis.

**Quiet boundary:** In dynamic analysis, the application of boundaries to the model may cause the applied propagating waves to reflect back into the model. Using

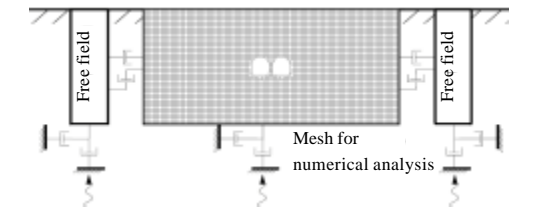


Fig. 5: Numerical model and boundary condition for dynamic analysis

 Table 1: Soil and earthquake properties used in the analysis

 Soil and earthquake parameters
 Value

 Peak ground acceleration at surface
 0.57 g

 Density of medium
 2600 kg m<sup>-3</sup>

 Poisson's ratio of medium
 0.32

 Modulus of elasticity of medium
 2554 MPa

 Peak particle velocity associated with S-waves
 610 m sec<sup>-1</sup>

a larger model may reduce this problem but consequently, a large computational time becomes a problem. An alternative is to use quiet (absorbing) boundary to overcome the problem. Lysmer and Kuhlemeyer (1969) suggested quiet boundary. Quiet boundary runs in the time domain and was based on the use of independent dashpots in the normal and shear directions applied at the model boundaries.

Quiet boundary is best suited for dynamic source applied within a grid. It should not be used along the side boundaries of a model when the dynamic source is applied at the top or bottom boundaries because the propagating wave will leak out of the side boundaries. For this case, free field boundary should be used (Itasca, 1999).

**Free field boundary:** The purpose of using free field boundary is similar to that of Quiet boundary in that it is used so that the outward waves propagating from inside the model can be properly absorbed by the side boundaries.

Free field boundary supplies similar conditions to that of an infinite model. A one-dimensional column width is created adjacent to the side boundaries of the model and are coupled each other by viscous dashpots.

Baseline correction: Baseline correction usually applies only to complex waveforms derived, for example, from field measurements. When using a simple, artificial waveform, it is easy to arrange the process of generating the waveform to ensure that the final displacement is zero. Usually, in dynamic analysis, the input wave is an acceleration record. A baseline correction procedure can be used to force both the final velocity and displacement to be zero. Earthquake engineering texts should be consulted for standard base-line correction procedures (Itasca, 1999).

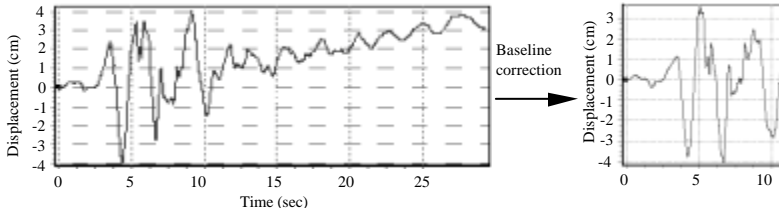


Fig. 6: Procedure of baseline correction

This can be done by applying a fixed velocity to the mesh to reduce the residual displacement to zero (Fig. 6). This action will not affect the mechanics of the deformation of the model (Fakhimi, 1997; Itasca, 1999).

Wave transmission: Numerical distortion of the propagating wave can occur in a dynamic analysis as a function of the modelling conditions. Both the frequency content of the input wave and the wave-speed characteristics of the system will influence the numerical accuracy of wave transmission. Kuhlemeyer and Lysmer (1973) show that for accurate representation of wave transmission through a numerical model, the spatial element size, l, must be smaller than approximately one-tenth to one-eighth of the wavelength associated with the highest frequency component of the input wave:

$$1 \le \frac{\lambda}{8 - 10} \tag{1}$$

where,  $\lambda$  is the wavelength associated with the highest frequency component that contains appreciable energy.

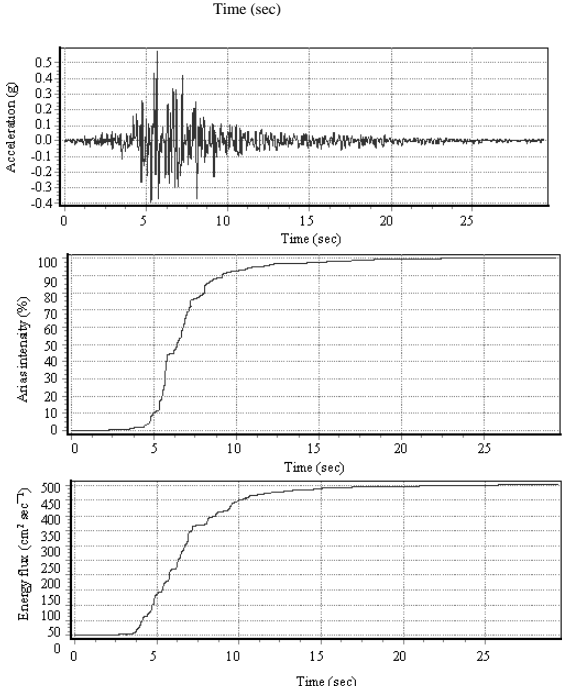
For dynamic input with a high peak velocity and short rise-time, the Kuhlemeyer and Lysmer (1973) requirement may necessitate a very fine spatial mesh and a corresponding small time step. The consequence is that reasonable analysis may be prohibitively time and memory-consuming.

This problem can be overcome by filtering the input time history and by removing the high frequency components. By filtering, the history and removing high frequency components, a coarser mesh may be used without significantly affecting the results (Fig. 7).

The difference in power between unfiltered and filtered input is less than 1%. Table 2 shows the difference in parameters between unfiltered and filtered inputs.

In this study, the seismic loading was represented by upward propagation of plan wave, shear or S-wave. The seismic record was corrected based on the power spectrum specified by Earthquake Design Spectra Code for Iran (1999).

Figure 5 shows the typical modelling mesh used in this study. The plane strain condition is assumed and the



20

25

Fig. 7: Kozani earthquake accelerogram recorded, total energy released and definition of the parameters

Table 2: Difference in parameters between unfiltered and filtered inputs				
Parameters	Unfiltered	Filtered		
Maximum velocity (cm sec-1)	23.725	23.73		
Maximum displacement (cm)	4.08	4.04		
$V_{max}/A_{max}$ (sec)	41.309	39.639		
Arias intensity (m sec <sup>-1</sup> )	2.0975	2.097		
Characteristic Intensity (Ic)	0.096	0.096		
Specific energy density (cm <sup>2</sup> sec <sup>-1</sup> )	503.73	503.43		
Acceleration spectrum intensity (g)	0.427	0.43		
Velocity spectrum intensity (cm)	117.38	115.95		

Table 3: The results of the numerical analysis (small twin tunnels)					
Point	$T_{max}(N)$	M <sub>max.</sub> (Nm)	$V_{max}$ (N)		
A	48E4	6E4	-19E4		
В	70E4	40E4	25E4		
C	67E4	20E4	22E4		
D	130E4	29E4	-45E4		
E	200E4	28E4	-59E4		
F	69E4	2.5E4	-49E4		

lining is modeled by a series of continuous flexural beam elements. The lining is assumed to be linear elastic material.

Figure 9-12 present the time histories of axial forces at various key points (Fig. 8) of the roof, walls and floor of the tunnel.

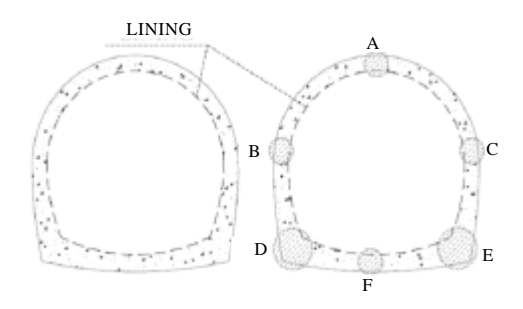


Fig. 8: Selected points to monitor the history of force in the lining (twin tunnels)

Table 4: The results of the numerical analysis (big section tunnel)

Point	$T_{max.}(N)$	M <sub>max.</sub> (Nm)	V <sub>max</sub> (N)
A	125E4	30E4	15E4
В	175E4	40E4	15E4
C	230E4	35E4	10E4
D	160E4	19.5E4	20E4
E	130E4	33E4	10E4
F	310E4	90E4	91E4
G	300E4	150E4	105E4
<u>H</u>	52E4	33E4	4E4

The results of the numerical analysis of dynamic analysis for Esfahan subway twin tunnels are shown in Table 3

The results of the numerical analysis of dynamic analysis for big section tunnel (Fig. 13) are shown in Table 4.

# COMPARISON OF NUMERICAL AND CLOSED FORM SOLUTION

Review of closed form solution: Ovalling deformations on circular tunnel are produced by wave propagation perpendicular to tunnel axis and are therefore designed for in transverse direction (typically under 2D, plane-strain conditions). According to studies made, propagation of vertical shear wave (SV); which cause vibration in horizontal direction are most effective on producing ovalling deformation around tunnel (Hashash *et al.*, 2001).

For a deep tunnel in homogeneous soil or rock, Newmark's simple method may give intellectual assessment of such deformations around tunnel free-field maximum shear strain is obtained as following accordingly (Hashash *et al.*, 2001):

$$\gamma_{\text{max}} = \frac{V_s}{C_s} \tag{2}$$

where,  $C_s$ , shear wave velocity and  $V_s$ , particle shear wave velocity.

By using free field maximum shear strain, produced free field diametric deflection around tunnel can be obtained in two forms (Hashash *et al.*, 2001):

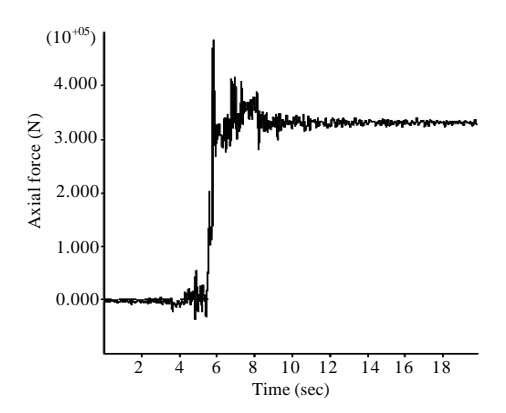


Fig. 9: Plot of axial force versus time at point A

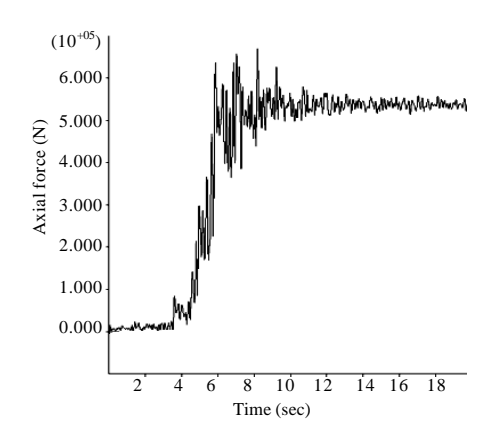


Fig. 10: Plot of axial force versus time at point B

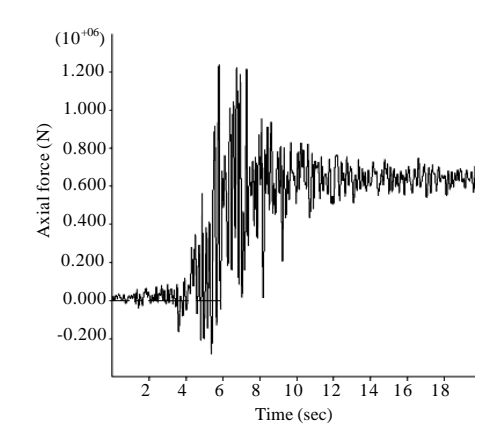


Fig. 11: Plot of axial force versus time at point D

Assuming no presence of tunnel cavity in the ground the ovalling effects from ground, in which case the diametrical strain is a function of maximum free field strain only

$$\Delta d_{\text{free field}} = \pm \frac{\gamma_{\text{max}}}{2} d \tag{3}$$

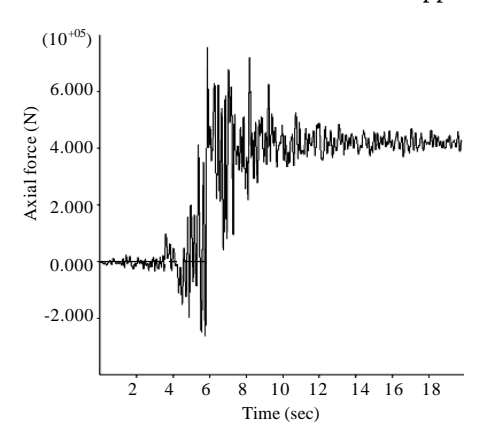


Fig. 12: Plot of axial force versus time at point F

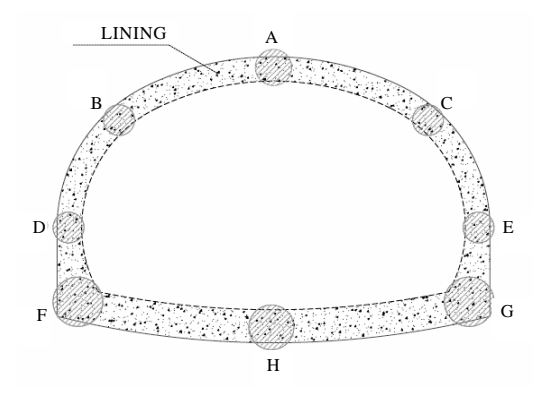


Fig. 13: Selected points to monitor the history of force in the lining

Ground deformation occurs in the presence of a cavity due to tunnel excavation, in which case the diametrical strain will be

$$\Delta d_{\text{free field}} = \pm 2\gamma_{\text{max}} d(1-\nu_{\text{m}}) \tag{4}$$

where,  $\mu_m$ , the Poison's ratio of the ground material and d, diameter or equivalent diameter of tunnel. Both of these equations assume the absence of the lining, therefore, ignoring tunnel-ground interaction.

This deformation is much greater in the case where the presence of the tunnel is included compared to the case where only the continuous ground deformation is assumed. In most cases, the lining ground interaction has to be taken into account.

In case of tunnel in soft ground, the above relationships do not consider the real behavior of the tunnel. In a case of rigid lining no deformation can be produced by the ground and for a flexible lining, on the other hand interaction between lining and ground exists. In this regard, flexibility and compressibility ratio suggested by Peck *et al.* (1972) based on earlier study by Hoeg (1968) can be used to take into account this factor (Hashash *et al.*, 2001):

$$C = \frac{E_m (1-v_1^2)r}{E_1 t (1+v_m) (1-2v_m)}$$
 (5)

$$F = \frac{E_{m} (1-v_{1}^{2})r^{3}}{6E_{I}I(1+v_{m})}$$
 (6)

where, F is flexibility ratio, C is the compressibility ratio,  $E_m$  is modulus of elasticity of the medium,  $E_1$  is modulus of elasticity of tunnel lining, I is the moment of inertia of the tunnel lining (per unit width) and r and t is the radius and thickness of lining. If F<20, interaction between lining and ground must be taken into account, otherwise free field approach explained above can be used. According to Wang (1993) solution (Hashash *et al.*, 2001):

$$T_{\text{max}} = \pm \frac{1}{6} K_{1} \frac{E_{\text{m}}}{(1 + \nu_{\text{m}})} r \gamma_{\text{max}}$$
 (7)

$$M_{\text{max}} = \pm \frac{1}{6} K_1 \frac{E_m}{(1 + v_{\perp})} r^2 \gamma_{\text{max}}$$
 (8)

$$\frac{\Delta d_{lining}}{\Delta d_{\text{doc, fold}}} = \frac{2}{3} K_1 F \tag{9}$$

where,  $T_{\text{max}}$  is maximum thrust in tunnel lining,  $M_{\text{max}}$  is maximum bending moment in tunnel lining,  $\Delta d_{\text{lining}}$  is the lining diametric deflection and  $K_1$  is full-slip lining response coefficient.

$$K_1 = \frac{12(1-v_m)}{2F + 5-6v_m} \tag{10}$$

This solution is based on full-slip assumption between lining and ground. This assumption is valid only for the case of very soft soil or earthquake of high intensity. In many situation condition of partial or no-slip exist. For trust force in lining (T), assumption of no-slip between lining and soil is acceptable and following relationship is suggested (Hashash *et al.*, 2001):

$$T_{\text{max}} = \pm \, K_2 \frac{E_{\text{m}}}{2(l+\nu_{\text{m}})} \, r \gamma_{\text{max}} \tag{11} \label{eq:Tmax}$$

In which:

$$K_{2} = \frac{F[(1-2v_{m})-(1-2v_{m})C] - \frac{1}{2}(1-2v_{m})^{2} + 2}{F[(3-2v_{m})+(1-2v_{m})C]} + C\left[\frac{5}{2}-8v_{m}+6v_{m}^{2}\right] + 6-8v_{m}}$$
(12)

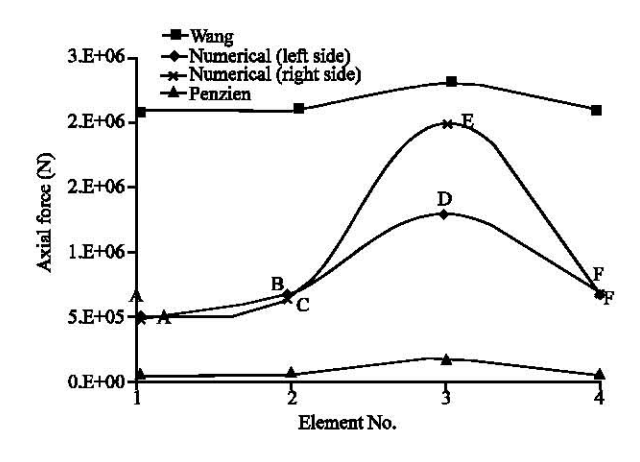


Fig. 14: Comparison of axial force distribution (small twin tunnels)

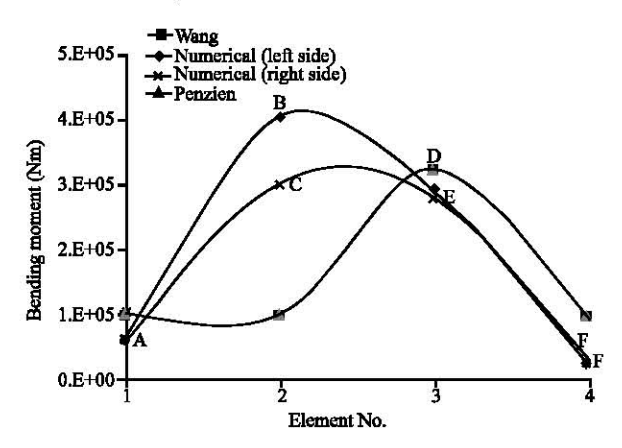


Fig. 15: Comparison of bending moment distribution (small twin tunnels)

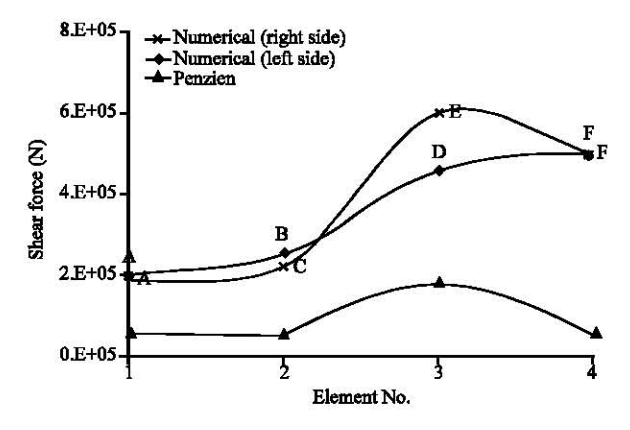


Fig. 16: Comparison of shear force distribution (small twin tunnels)

Penzien (2000) developed similar analytical solutions for thrust, shear and moment in the tunnel lining due to racking deformations. Assuming full slip condition,

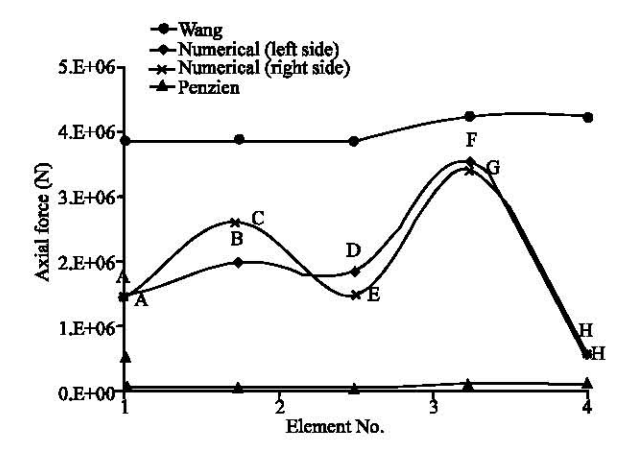


Fig. 17: Comparison of axial force distribution (big section tunnel)

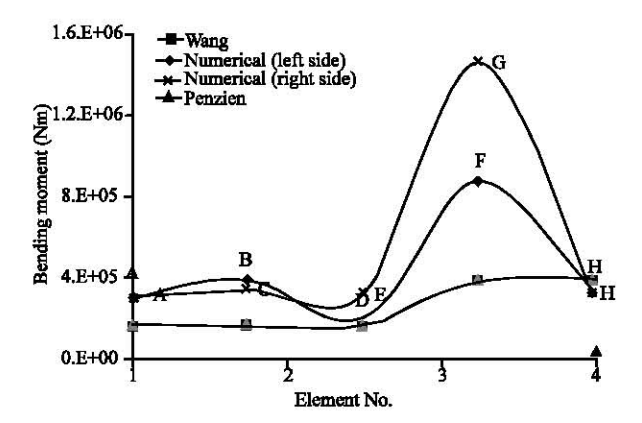


Fig. 18: Comparison of bending moment distribution (big section tunnel)

solutions for thrust, shear in circular tunnel linings caused by soil-structure interaction during a seismic event are expressed as (Hashash *et al.*, 2001):

$$\Delta d_{\text{lining}}^{n} = R^{n} \frac{\gamma_{\text{max}} d}{2}$$
 (13)

$$T_{\text{max}} = \pm \frac{12 E_l I \Delta d_{\text{liming}}^n}{d^3 (1 \! - \! \nu_l^2)} = \pm \frac{6 E_l I R^n \! \gamma_{\text{max}}}{d^2 (1 \! - \! \nu_l^2)} \tag{14} \label{eq:Tmax}$$

$$M_{\text{max}} = \pm \frac{6 E_I \Delta d_{\text{lining}}^n}{d^3 (1 \! - \! \nu_I^2)} = \pm \frac{3 E_I I R^n \! \gamma_{\text{max}}}{d^2 (1 \! - \! \nu_I^2)} \tag{15} \label{eq:max}$$

$$V_{\text{max}} = \pm \frac{24 E_{l} I \Delta d_{\text{lining}}^{n}}{d^{3} (1 \! - \! v_{l}^{2})} = \pm \frac{12 E_{l} I R^{n} \gamma_{\text{max}}}{d^{2} (1 \! - \! v_{l}^{2})} \tag{16} \label{eq:Vmax}$$

The lining-soil racking ratio under normal loading only is defined as (Hashash *et al.*, 2001):

Table 5: Comparison of numerical results with analytical solutions (small twin tunnels)

Numerical analysis		Wang (1993) method		Penzien (2000) method		
Variables	A,B,C,F ( $t = 40 \text{ cm}$ )	D,E ( $t = 60 \text{ cm}$ )	t = 40  cm	t = 60  cm	t = 40  cm	t = 60  cm
Maximum thrust, T <sub>max.</sub> (N)	67E4	170E4	208.3E4	229.4E4	5.58E4	18.2E4
Maximum moment, M <sub>max.</sub> (Nm)	40E4	28E4	9.79E4	32.0E4	9.79E4	32.0E4
Maximum shear, V <sub>max.</sub> (N)	25E4	59E4	-	-	5.58E4	18.2E4

Table 6: Comparison of numerical results with analytical solutions (big section tunnel)

	Numerical analysis		Wang (1993) method		Penzien (2000) method	
Variables	A,B,C,F (t = 60 cm)	D,E $(t = 80 \text{ cm})$	t = 60 cm	t = 80  cm	t = 60  cm	t = 80  cm
Maximum thrust, T <sub>max.</sub> (N)	230E4	310E4	384.4E4	416.7E4	4.75E4	11.2E4
Maximum moment, Mmax. (Nm)	40E4	150E4	16.65E4	39.2E4	16.65E4	39.2E4
Maximum shear, V <sub>max.</sub> (N)	20E4	52E4	-	-	4.75E4	11.2E4

$$R^{n} = \frac{4(1 - v_{m})}{(\alpha^{n} + 1)} \tag{17}$$

$$\alpha^{\rm n} = \frac{12 E_{\rm I} I (5-6 v_{\rm m})}{d^3 G_{\rm m} (1-v_{\rm I}^2)} \eqno(18)$$

where,  $\Delta d^n_{lining}$  is the lining diametric deflection under normal loading,  $R^n$  is lining-soil racking ratio under normal loading and  $G_m$  is shear modulus of soil or rock medium.

In the case of no-slip condition, the equations are presented as (Hashash *et al.*, 2001):

$$\Delta d_{\text{liming}} = R \frac{\gamma_{\text{max}} d}{2}$$
 (19)

$$T_{\text{max}} = \pm \frac{24 E_1 I \Delta d_{\text{liring}}}{d^3 (1 - v_1^2)} \tag{20} \label{eq:Tmax}$$

$$M_{_{max}}=\pm\frac{6E_{_{I}}\mathrm{L}\Delta d_{_{liring}}}{d^{2}(1-\nu_{_{I}}^{2})}=\pm\frac{3E_{_{I}}\mathrm{IR}\gamma_{_{max}}}{d(1-\nu_{_{I}}^{2})} \tag{21}$$

$$V_{_{\text{max}}} = \pm \frac{24 E_I I \Delta d_{_{\text{liring}}}}{d^3 (I - v_I^2)} = \pm \frac{12 E_I I R \gamma_{_{\text{max}}}}{d^2 (I - v_I^2)} \tag{22} \label{eq:22}$$

where, R is the lining-soil racking ratio:

$$R = \pm \frac{4(1 - v_m)}{(\alpha + 1)} \tag{23}$$

$$\alpha = \frac{24E_1I(3-4v_m)}{d^3G_m(1-v_1^2)} \tag{24}$$

The results of comparison between numerical and analytical solution: The numerical results presented in the above were compared with the analytical solutions proposed by Wang (1993), Penzien (2000) and Hashash *et al.* (2001).

The results of the numerical analysis compared to analytical solutions in Table 5 and 6.

Figure 14-16 show the comparison of axial force, bending moment and shear force distributions for two lining thickness, respectively. Figure 17-18 show the comparison of axial force, bending moment for big section tunnel. Figure 18 shows that analytical value in points G and F are very lower than numerical results.

The numerical results of axial force distribution are slightly lower than Wang (1993) solution results. The Penzien (2000) solution results of shear force distribution in points D, E are very lower than numerical results (Fig. 16).

### CONCLUSION

The safety of tunnel lining in Esfahan subway has been evaluated by using a numerical analysis. The numerical studies were obtained by time domain analysis using accelerogram generated according to prescribed seismic hazard analysis (SHA) and power spectra.

The available analytical solutions for the seismicinduced ovalling of the lining in a circular tunnel were investigated by comparing the results of thrust and moment with those of the numerical analysis (horseshoe tunnel).

The solutions by Penzien (2000) and Wang (1993) provided identical results of moment, whereas differ in the axial force distribution. The solution by Penzien (2000) results in underestimate of axial force distribution.

Although the analytical procedure in this study is limited in scope, it appears to be useful for a preliminary design of tunnel linings to estimate the seismic effect.

## ACKNOWLEDGMENTS

The authors wish to thank Haraz Rah Consulting Engineers Group and Sazbon Pajooh Consulting Engineers for providing access to the tunnel geotechnical data of the Esfahan metro tunnels project. The help by Eng. S. Bagherzadeh, Eng. R. Mikaeil and Eng. M. Nakhaei is kindly acknowledged.

### REFERENCES

- Amiri, G.G., R. Motamed and H.R. Es-haghi, 2003. Seismic hazard assessment of metropolitan Tehran, Iran. J. Earthquake Eng., 7: 347-372.
- Fakhimi, A.A., 1997. Theory and Manual of CA2 Software. Version II. Center for Housing and Building Research of Iran, Iran.
- Hashash, Y.M.A, J.J. Hook, B. Schmidt and J.C. Yao, 2001. Seismic design and analysis of underground structures. Tunneling Underground Space Technol., 16: 247-293.
- Hoeg, K., 1968. Stresses against underground structural cylinders. J. Soil Mech. Founds Div. ASCE, 94: 833-858.
- Iranian Code of Prac Publication, 2003. Tice for Seismic Resistant Design of Buildings, 1999. Standard No. 2800, 2nd Revision, Building and Housing Research Center, Iran, (In Persian).
- Itasca Con, G., 1999. Fast lagrangian analysis of continua. Version 4.10 User's Manual, Minneapolis.
- Kramer, S.L., 1996. Geotechnical Earthquake Engineering. 1st Edn., Prentice Hall, New Jersey, ISBN-13: 9780133749434, pp. 653.

- Kuhlemeyer, R.L. and J. Lysmer, 1973. Finite element method accuracy for wave propagation problems. J. Soil Mech. Founds Div. ASCE, 99: 421-427.
- Lysmer, J. and R.L. Kuhlemeyer, 1969. Finite dynamic model for infinite media. J. Eng. Mech. Div. ASCE, 95: 859-877.
- Newmark, N.M. and W.J. Hall, 1982. Earthquake Spectra and Design. 1st Edn., EERI Monograph, Earthquake Engineering Research Institute, Berkeley, California. ISBN-13: 978-0943198224, pp. 103.
- Peck, R.B., A.J. Hendron and B. Mohraz, 1972. State of the art in soft ground tunneling. Proceedings of the Rapid Excavation and tunneling Conference American Institute of Mining, Metallurgical and Petroleum Engineering, 1972 New York, pp. 259'-286.
- Penzien, J., 2000. Seismically induced racking of tunnel linings. Int. J. Earthquake Eng. Struct. Dynamics, 29: 683-691.
- St John, C.M. and T.F. Zahrah, 1987. A seismic design of underground structures. Tunneling Underground Space Technol., 2: 165-197.
- Tavakoli, B. and M.G. Ashtiany, 1999. Seismic hazard assessment of Iran. The Global Seismic Hazard Assessment Program (GSHAP), Annali Di Geo-Sica: 42
- Wang, J.N., 1993. Seismic Design of Tunnels: A State-ofthe-Art Approach. 1st Edn., Parsons Brinckerhoff Quade and Douglas, Inc., New York.